FIBER REINFORCED POLYMER C-FRAMES WITH INTEGRATED DAMPING TREATMENT FOR AEROSPACE FUSELAGE APPLICATIONS

Caroline Hofer
Technische Universität München, Boltzmannstraße 15, 85748 Garching bei München, Germany

Abstract

This work was initiated by MAAXIMUS, an European research program for composite aircrafts, and was conducted at the Center of Structure Technologies of the ETH Zurich. It deals with the integration of the vibration damping function into structural fuselage components. The objective is to investigate the vibro-acoustic and mechanical properties of carbon fiber reinforced polymer C-frames with integrated viscoelastic layer manufactured by the RTM process. The dynamic and numerical analyses show on the one hand that the finite element updating by means of the modal strain energy method does not improve the correlation of simulation and test results in the same way as for more simple geometries. On the other hand they indicate that the viscoelastic layer does not noticeably improve the overall damping performance. The static tests show different results. In the specially developed “step" test the profile with viscoelastic layer performs worse than the profile without viscoelastic layer. However, the four-point bending test reveals higher mechanical properties for the profile with viscoelastic layer. This study also includes the design and the construction of a RTM tool, that has been used for the manufacturing of profiles with and without damping treatment.

1. INTRODUCTION

MAAXIMUS (More Affordable Aircraft through eXtended, Integrated and Mature nUmerical Sizing) [1], an aeronautic project funded by the European Commission under the Seventh Framework Programme, aims at achieving the reduction of development costs and time, non-recurring costs, aircraft weight and manufacturing and assembly costs by conducting research on two levels. While the Virtual Platform has the objective to improve simulation techniques for the development of composite aircraft structures, the Physical Platform deals with the manufacturing and assembly of a composite fuselage barrel. Within MAAXIMUS Dassault Aviation focuses his work on a mini-barrel (see the left picture of BILD 1) in collaboration with the Centre of Structure Technologies (IMES-ST) from the ETH Zurich and Constructions Industrielles de la Méditerranée (CNIM). This mini-barrel shall be assembled from an ovoid section with co-cured stringers from CNIM, curved C-frames with integrated damping from ETH and composite window frames from Dassault Aviation.

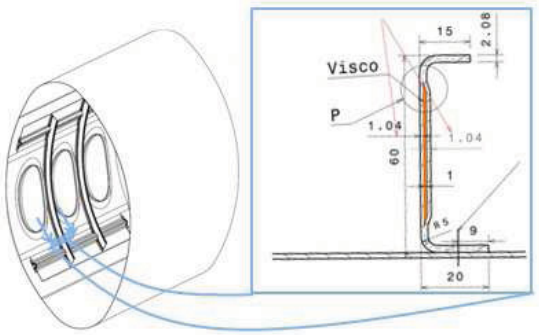

BILD 1. Technical drawing of the mini-barrel and the C-frame cross section

The basis of this work is the MAAXIMUS task of ETH to compare the structural response and damping performance of different C-frames manufactured with RTM.

To achieve this goal, first a method to perform vibro-acoustic tests on a thin-walled open beam using an aluminum frame must be evaluated. It includes a comparison with FE models. Then a tool for the manufacturing of straight profiles with a length of 600 mm and two different cross sections based on the RTM process shall be designed. The cross section with damping treatment is prescribed by Dassault Aviation, as one can see in the right picture of BILD 1. Third both cross sections will be tested by performing static and dynamic tests to assess the performance of the design solution. The fourth objective is to develop accurate FE models, which will be used for optimization of type and position of the damping treatments according to the results before to maximize damping and mechanical performance with the lowest weight increase.

2. LITERATURE REVIEW

Damping is physically considered as the conversion of vibration energy into heat. The existing damping methods can be classified as either active or passive damping, while the second one is based on friction effects by additionally applying special materials to the vibrating structure. One group of these special materials are the viscoelastic materials, whose stress-strain relation can be described according to [2] by the following equation, where $E(0)$ is called relaxation function and τ is the integration variable:

$$\sigma = \varepsilon(t)E(0) + \int_0^t \varepsilon(t-\tau)\frac{\partial E}{\partial \tau}(\tau)d\tau \quad (1)$$

Assuming a harmonic excitation $\varepsilon(t) = \varepsilon_0 e^{i\omega t}$ and $t \to \infty$, it

can be written in its original form

(2) $\sigma(t) = E^* \varepsilon(t)$

with the complex modulus E^*, which can be described by the storage modulus E' and the loss modulus E'':

(3) $E^* = E(0) + \int_0^\infty e^{-i\omega t} \frac{\partial E}{\partial \tau}(\tau) d\tau = E'(\omega) + iE''(\omega)$

The ratio of both moduli is called the loss factor η:

(4) $\eta = \frac{E''}{E'}$

Ungar and Kerwin [3] declared the loss factor to be the best parameter to analyze the damping performance of an arbitrary system, because it is not based on linear single-degree-of-freedom systems and constant parameters, but on energies, which also allow non-linear systems with frequency-dependent parameters. They stated that the loss factor can also be determined as ratio of the sum of different material loss factors multiplied with the related stored energies to the total stored energy. This analytical formula is the mathematical basis of the modal strain energy method (MSEM), which was combined with the finite element method by Johnson, Kienbaum and Rogers [4]. The resulting equation describes the loss factor of the r'th mode of the composite structure $\eta^{(r)}$ as a function of the material loss factor for the viscoelastic material η_v, the r'th mode shape vector $\tilde{\phi}^{(r)}$, the subvector $\tilde{\phi}_e^{(r)}$ formed by deleting all entries not corresponding to the motion of the nodes of the e'th viscoelastic element, the element stiffness matrix $\tilde{K}_e$ of the e'th viscoelastic element, the stiffness matrix $\tilde{K}$ of the entire composite structure and the number n of viscoelastic elements in the model:

(5) $\frac{\eta^{(r)}}{\eta_v} = \frac{\sum_{e=1}^{n} \tilde{\phi}_e^{(r)} \tilde{K}_e \tilde{\phi}_e^{(r)}}{\tilde{\phi}^{(r)T} \tilde{K} \tilde{\phi}^{(r)}}$

One method to calculate the modal loss factor from dynamic test results, is the “n dB" method, described in [5]:

(6) $\eta = \left(\frac{1}{\sqrt{10^{n/20} - 1}} \right) \frac{\Delta f}{f}$

Here, f is the measured response function, n is a value, that must be chosen between 0.5 and 3 and Δf must be calculated by deducting the two frequencies at the values of the response curve with n dB less than the resonance value.
Basing on the before mentioned methods, Lepoittevin [6] developed a finite element method for predicting the resonance frequencies and loss factors for damped structures under free-free boundary conditions, based on a suspension modeling with spring-damper elements and the updating of their stiffness and damping coefficients corresponding to vibration test results.

3. DYNAMIC ANALYSIS OF A THIN-WALLED OPEN BEAM

Due to the fact, that the dynamic behavior of structures with shapes unlike plates were hardly investigated so far, the first part of this work aims at the experimental and numerical identification of the C-frame's eigenmodes and the consistency of both approaches. To ensure a stepwise validating approach, these analyses were conducted with an aluminum C-frame, having the same measures as Dassault Aviation requires but only with a thickness of 1.5 mm.

3.1. Experimental Analyses

The experiments are conducted with a test set-up, that provides nearly free-free boundary conditions to the specimen (see BILD 2).

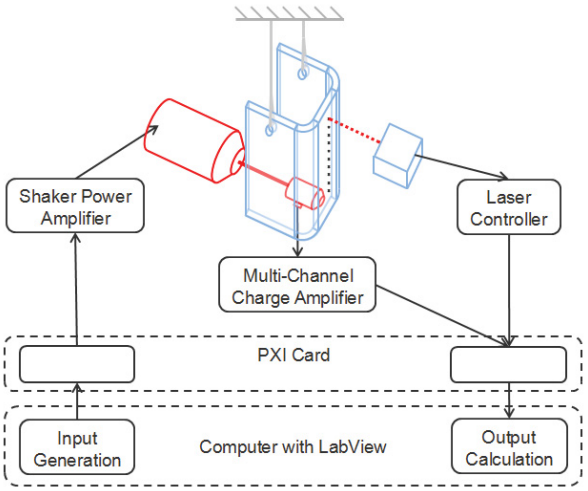

BILD 2. Set-up of the vibro-acoustic test

To properly work out all eigenmodes and especially their exact mode shapes a C-frame made of aluminum is suspended and excited in different configurations. The result of the investigation of both the frequency response functions and the plot of the three-dimensional mode shapes is that two different configurations are needed to be able to analyze both, the mode shapes of the web and the mode shapes of the flanges. The left configuration in BILD 3 is used to excite the bending modes of the web and with the right configuration the torsion modes of the flanges can be excited.

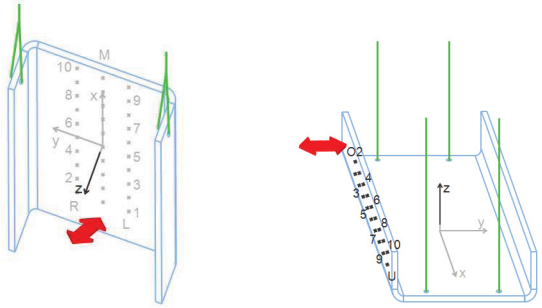

BILD 3. Test set-up of the two configurations

The reason for the necessity of the second suspension configuration is that with the first configuration the three dimensional mode shapes of the flanges are not measurable. This may result from the fact, that the suspension damps the vibration of the surface and

therefore the absolute vibration amplitude is smaller than the one of the surface without suspension. Assuming now, that the measured surface is not perfect, the laser beam is not exactly perpendicular to the surface and the laser measurement itself is noisy, these errors higher influence a smaller amplitude than a higher one. Furthermore even without the damping influences of the suspension, the deformations of the flanges are generally smaller than the one of the web. Furthermore they move not only in laser direction but also in the plane perpendicular to it.

3.2. Numerical Analyses

The numerical analyses of the aluminum profile in the first configuration with and without constrained layer damping treatment are carried out with ANSYS 12.0.
The aluminum profile and the viscoelastic layer of the constrained layer damping treatment are modeled by *solid186* elements. For the excitation of the frame, consisting of shaker, stringer, impedance head and joint, the *beam4* element is used. The suspension of the frame, which is in reality a thread, is approximated with the element *combin14* in its three-dimensional, longitudinal configuration.
Due to the approximately free-free boundary conditions only the upper ends of the suspensions is taken to be clamped and the last node of the excitation part is modeled as a floating bearing with the displacement in lengthwise direction as the only degree of freedom.
Although a small sensitivity analysis, a finite element updating dealing with coefficient adaption according to Lepoittevin [6] and an extended updating regarding element type and configuration adaption are carried out, the best numerical evaluated loss factor is still 45% lower than the experimental measured one. The reason might either be an incomplete model updating or the impossibility to use the modal strain energy method for complex geometries.

4. MOULD CONSTRUCTION

Beside the normal size and manufacturing process requirements the tool for producing the straight C- frames with and without viscoelastic layer by resin transfer molding must fulfill also additional demands regarding the accurate controlling and monitoring of the injection. This includes the placement of several sensors.
The resulting mould design consists of eleven parts, is made from S355J2G3 and can be seen in BILD 4.

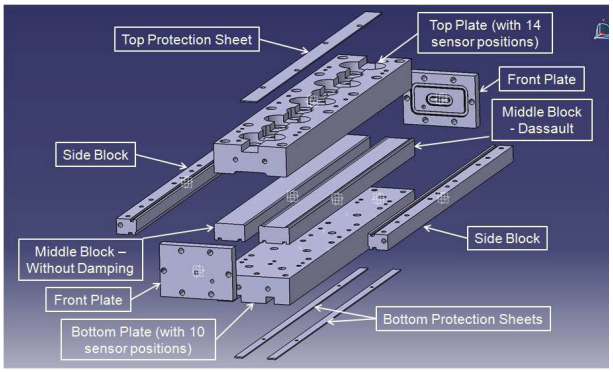

BILD 4. Exploded drawing of the mould

Here the bottom plate forms the lower limit of the frame's flanges, or respectively of the resin channels, which follow on the flanges and which are necessary to make sure that the resin can spread homogeneously from the injection channel to the outlet channel and wet all fibers. The bottom plate can include up to ten sensors for observing each resin channel with five sensors, equally distributed over the mould length.
The top plate forms the upper limit of the C-frames, including the outer edges. It provides fourteen sensor positions, of which ten are equally distributed over the length in pairs and placed as close as possible to the edges, where the resin arrives, and the rest is located on the center line of the profile. All sensors are connected by one broad channel for the sensor cables.
The two side blocks are the outer limits of the flanges of the profile and the resin channels.
The two front plates close the mould in the longitudinal direction and provide the mounting points for the hose adapters.
The middle blocks, one for the profile without damping layer and one for the profile with damping layer according to Dassault Aviation requirements, give the frames its' inner shape.
Furthermore there are two bottom protection sheets and one top protection sheet, which are meant to close the cable channels of the bottom plate and the top plate.

5. MANUFACTURING WITH THE RTM PROCESS

The RTM manufacturing process consists of five main steps, which are the tool preparation, the RTM process preparations, the resin injection, the curing and the post processing.
First the mould will be treated with semi-permanent mould release agent and preassembled to two parts. Next, the fabrics and – in case of manufacturing a C-frame with damping treatment – also the viscoelastic layer must be cut and draped in a quasi-isotropic layer set-up, provided by DASSAV ([0₹90°,+/-45°,0₹90°,+/.45₹]s or [(0₹90°,+/ - 45°,0₹90°,+/-45₹)s, VEL]). At last the mould is close d by deep-drawing the fibers and sealed with O-rings and sealing tape.
Secondly the RTM process must be prepared by connecting the heatable pressure pot and the outlet pressure pot to the mould with high temperature hoses, heating the mould in the press at 125℃ for 60 minu tes with 40 to 50 kN pressure and heating the resin under vacuum at 80℃ for 35 minutes.
The resin injection itself is conducted under vacuum and 4 bar pressure.
Next the resin is cured at 180℃ for 180 minutes un der 3 bar pressure.
After several hours of passive cooling the mould can be disassembled (see BILD 5) and the frame can be cut to its final measures, as BILD 6 shows.

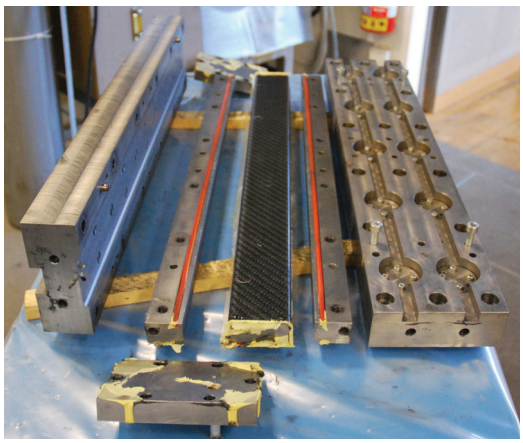

BILD 5. Disassembled mould

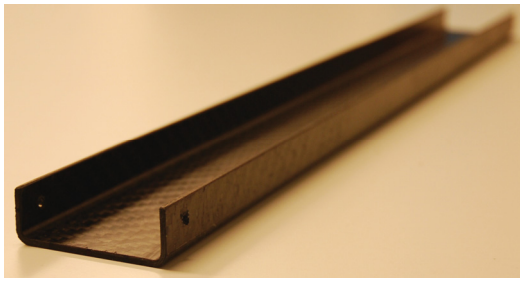

BILD 6. Carbon fiber reinforced polymer C-frame without viscoelastic layer manufactured by the RTM process

6. STATIC AND DYNAMIC TESTS

In order to compare the manufactured C-frames, especially the ones with and the ones without viscoelastic layer, several tests are performed. The first vibro-acoustic test of all profiles in the second configuration from chapter 3 reveals the differences due to the manufacturing process and evaluates the best-performing member of each group. Subsequently these two representatives are tested dynamically to also investigate the pure bending behavior of the C-frames, by suspending them in the related configuration. The other six profiles are used for the two static tests, the four-point bending test and the "step" test.

6.1. Vibro-Acoustic Rating Test

The results of the vibro-acoustic analysis of the four profiles without viscoelastic layer, which are the frequency response functions, the mean resonance frequencies of the five main modes and the mean loss factors of their peaks, evaluated by MATLAB using the "n dB" method, can be seen in BILD 7.
Although all four profiles show qualitatively the same frequency response function, the resonance frequencies diverge between 14 Hz for mode 1 and 30 Hz for mode 3. Whereby the fourth mode of profile 3 is not included into the calculations, because of its too high deviation in frequency and loss factor. Furthermore the loss factor of the second mode of profile 3 cannot be found in the table, because it is not even measurable with the "n dB" method setting n to 1. The reason for the behavior of profile 3 may result from the fact that opposite to all other beams, in case of profile 3 the thicker flange was excited and the thinner one was measured. So the lower eigenfrequencies could result from the higher mass of the left flange compared to the right flange. All other measures of profile 3 show no noticeable differences. Another necessary comment on BILD 7 regards the way of calculating the loss factors, which was carried out by analyzing every peak with the "n dB" method, setting n to 1, 2 and 3, and averaging the results to compensate measurement error related calculation faults. The loss factors of the profiles without viscoelastic layer are quite high, which is assumed to result from the internal damping of the CFRP material.

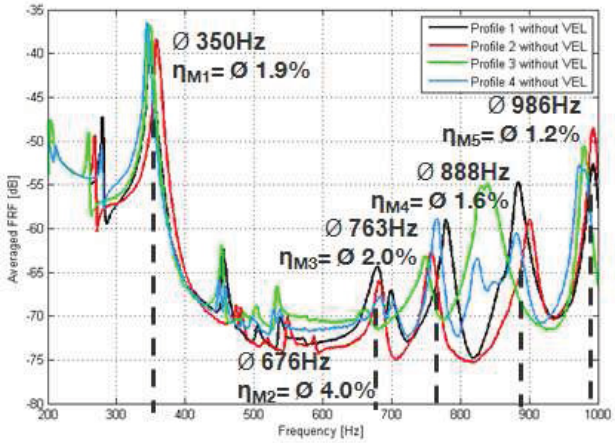

BILD 7. Frequency response function of four profiles without viscoelastic layer

In BILD 8 one can see the frequency response function of the four profiles with viscoelastic layer, the mean resonance frequencies of the four main modes and the related mean loss factors. These plots do not only show qualitatively the same course, but the deviation between highest and lowest resonance frequency of one mode lie between 0 Hz for mode 1 and 26 Hz for mode 3. This high value results from the fact that in this frequency range at least two eigenmodes interfere.

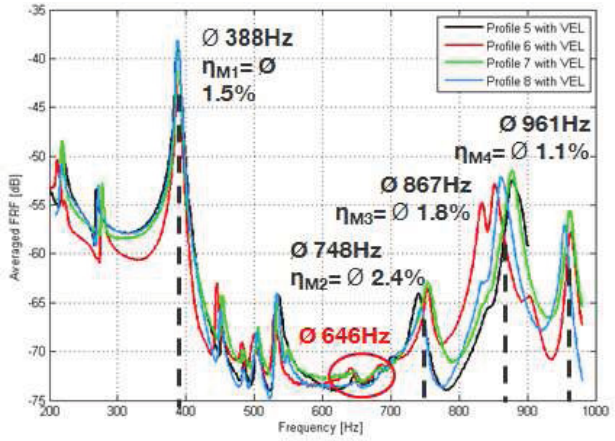

BILD 8. Frequency response function of four profiles with viscoelastic layer

Comparing the resonance frequencies of the profiles with and without viscoelastic layer, as TAB 1 shows, one can see that the first mode of the damped profile is higher than the undamped one, although the higher mass should decrease the frequencies. The reason could be that this mode is mainly influenced by torsion around the x-axis and the existence of the viscoelastic layer results in a torsional stiffness increase, because of the parallel axes theorem and the fact that the layers of the web around the viscoelastic layer act as a "closed profile". The lower loss factor (see TAB 2) indicates that the viscoelastic layer has

no damping influence, which means that it is not deformed in a significant way and resulting from the higher stiffness and the higher eigenfrequency, the loss factor decreases.
In contrary to the first mode, the following three or four modes behave as expected, assuming that the second mode has such a high loss factor that it is decreased 30 Hz to the hardly noticeable mode at 646 Hz. Then the third undamped mode corresponds to the 15 Hz lower mode 2 of the frequency response function with viscoelastic layer, as TAB 1 shows, mode 4 without viscoelastic layer and the damped mode 3 have a distance of 21 Hz and mode 5 of the undamped frequency response function belongs to the 25 Hz lower mode 4 of the profile with viscoelastic layer (VEL).

Mode	Profile without VEL	Profile with VEL	Difference
1	350 Hz	388 Hz	+38Hz (+10.9%)
2	676 Hz	646 Hz	-30Hz (-4.4%)
3	763 Hz	748 Hz	-25Hz (-3.3%)
4	888 Hz	867Hz	- 21Hz (-2.4%)
5	986 Hz	961 Hz	- 25Hz (-2.5%)

TAB 1. Comparison of resonance frequencies

This observation is also valid for the loss factors. In TAB 2 one can see an increase of 0.4% for the third undamped mode and the second damped mode, that corresponds to a relative increase of 20%. The next mode pair would result in an absolute loss factor increase of 0.2% and a relative increase of 12.5% and mode 5 of the profile without viscoelastic layer and mode 4 of the profile with viscoelastic layer would slightly decrease, absolute 0.1% and relative 8%. Whereby the loss factor of 1.2% for mode 5 is mainly caused by the higher-than-average loss factor of profile 4. Without this value mode 4 would only have a value of 1.0% and then also this last mode would be slightly better damped with viscoelastic layer than without.

Mode	Profile without VEL	Profile with VEL	Difference
1	1.9 %	1.5 %	- 0.4 %(- 21%)
2	4.0 %	-	-
3	2.0 %	2.4 %	+ 0.4 %(+ 20%)
4	1.6 %	1.8 %	+ 0.2 %(+12.5%)
5	1.2 %	1.1 %	- 0.1% (- 8.3%)

TAB 2. Comparison of loss factors

Altogether the damping performance of the viscoelastic layer at room temperature with the actual position and geometry and evaluated in its real operation configuration does not lead to a remarkable increase in damping, but even increases the stiffness of the profile, as the first mode showed.

6.2. Vibro-Acoustic Bending Test

Due to the low damping results of the chapter before, the vibro-acoustic bending test shall show, if this is also the case for the excitation of the web's pure bending modes. The test is carried out in the first configuration, evaluated in chapter 3, but because of the fact that the shaker, that was used for the previous measurements, is broken and therefore the comparability of the results is not fully ensured, only the first bending mode is investigated by using a bigger shaker.
The results in BILD 9 indicate that the viscoelastic layer reduces the resonance frequency of the first bending mode, because the increase in weight is higher than the increase in bending stiffness. Furthermore the loss factor is raised of about 0.6%, which corresponds to a relative increase of 60%.

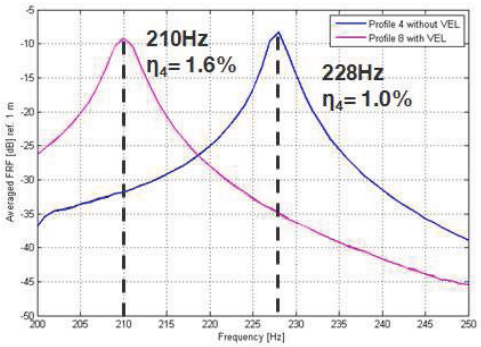

BILD 9. Frequency response function of the first bending mode of a profile with and without viscoelastic layer

Compared to the 12.5% and the 20% of the excitation in the second configuration, the damping efficiency for the bending mode is much higher. This fact supports the conclusion that the viscoelastic layer would perform better, if its positioning would be better adapted to the real operation behavior or if the C-frame would be changed in a way that the viscoelastic layer is higher deformed than in the current way. Practical realizations would be either to change the position of the viscoelastic layer, for example to integrate it in the flanges, because here the deformation is higher. The second possibility would be to modify the carbon fiber reinforced C-frame, for example by notching the inner CFRP layer of the web at positions corresponding to the mode shapes to increase the deformation of the viscoelastic layer.
Another predetermined reason for the low damping performance at room temperature is that the used viscoelastic layer is designed for aeronautical applications and has therefore its maximum damping performance at much lower temperatures.

6.3. Four-Point Bending Test

The bending test set-up consists of one bottom part, one top part and two mounting blocks (see BILD 10). Together with these blocks, on which the specimen should be fixed, the bottom plate provides the two lower mountings of the specimen, having a distance of 550mm. Both lock two rotational and two translational degrees of freedom. Therefore the specimen can only move in x-direction and rotate around its y-axis. The two circular blocks of the top part have a distance of 200 mm and are used to apply the bending force to the specimen. Due to an unplanned mode of failure during the first test run, the mounting

configuration was changed from configuration 1 to configuration 2.

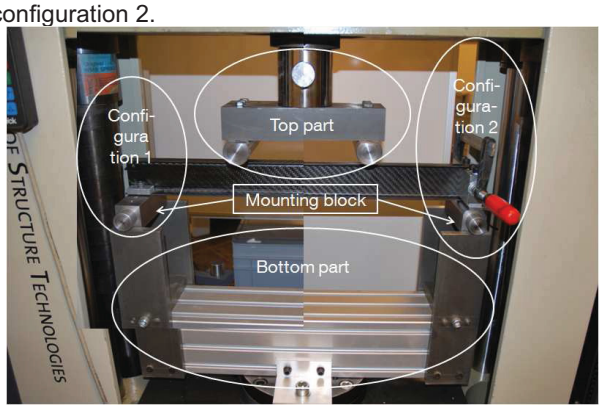

BILD 10. Test set-up of the four-point bending test

The behavior of both test specimen without viscoelastic layer, which leads to the failure in BILD 11, are almost the same. The web and the upper flange of the frame first tilt forwards under the bending load. As soon as the tensile stress in the upper flange is too high, the flange fails about 30 mm left of the its center and causes also a crack in the upper web. Next the test continues and the web tilts until web and lower flange fail at the same time.

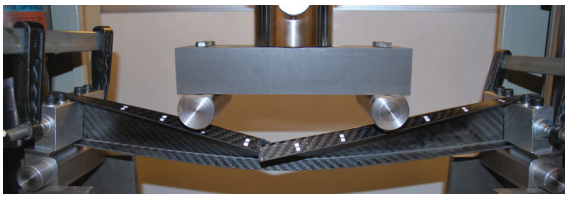

BILD 11. Four-point bending test of a profile without viscoelastic layer

BILD 12 shows the force-strain diagram for both frames, where the strain is given in mm. Although usually those graphs are converted into stress-strain diagrams by referring the length change to the original length and the applied force to the vertical cross-section surface of the not deformed specimen, this will not be carried out because of the complex shape of the cross-section. The basic behavior of both profiles is the same and the difference in the maximum force, which causes the fracture of the upper flange, results from the fact that in the first test the narrower flange was the upper flange and in the second test the broader was at the top. The difference of the forces, which caused the final failure of web and flange, is quite small, which shows that this force mainly depends on the bending strength of the web.

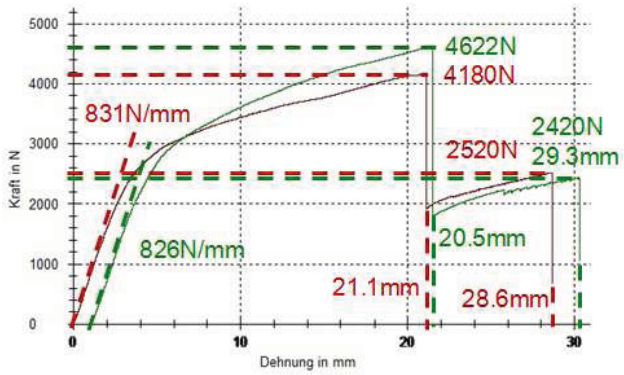

BILD 12. Force-strain diagram of the profiles without viscoelastic layer

The profiles with viscoelastic layer, having the failure as shown in BILD 13, behaved different than the profiles without viscoelastic layer. Here the web and the upper flange did not tilt as much as the frame without viscoelastic layer before the upper flange fails at the two upper mounting positions at the same time without affecting the web. Both the minor tilting and the failure of the flange on two points, are hints on a higher torsional stiffness of the web. Under the continuing force the web tilts for a comparable long time, due to a higher bending strength, until web and lower flange fail together at the same time.

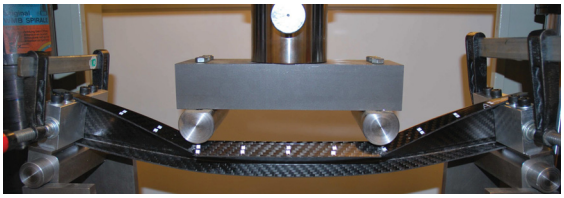

BILD 13. Four-point bending test of a profile with viscoelastic layer

The force-strain diagram in BILD 14 shows that the profiles with viscoelastic layer behave in the same way up to the failure of the upper flange. Afterwards the first profile continuously withstands the force until web and lower flange fail, but the web of the second one breaks in several steps before it and the lower flange completely fail.

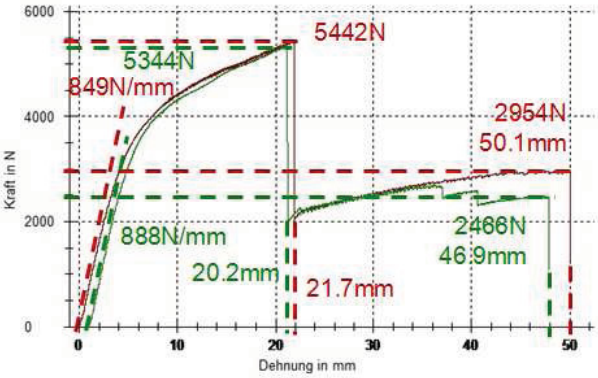

BILD 14. Force-strain diagram of the profiles with viscoelastic layer

The above-mentioned observations are supported by comparing the two force-strain diagrams, because the failure of the upper flange occurs at the same strain of about 21 mm for the profiles with and without viscoelastic layer, but the total failure of the profile without viscoelastic layer follows after another 8 mm and the profile with viscoelastic layer is bended additionally 27 mm.
Summarizing, one can say that the profile with viscoelastic layer has a higher torsional stiffness because of the high Young's modulus or spring rate. The higher maximum applicable force also indicates a higher bending strength against bending around the z-axis of about 22%. The bending strength of the web and the lower flange after the failure of the upper flange, is about 10% higher than the one of the profile without viscoelastic layer.

6.4. “Step” Test

The test set-up of the “step" test, as one can see in BILD 15, consists of the bottom plate, the “foot" and one top part, which is comprised of the machine interface, the “knee" and the “leg". The bottom plate provides first the

holes for fixing the profile in different positions relative to the “foot" and second it contains a mechanism to horizontally guide it. There are seven rows of holes with a distance of 20 mm in each direction, to be able to position the profile right under the foot suspension or in front and behind this line. The “foot" must be connected to the leg and the horizontal guide of the bottom plate. Due to initial problems at the bending test, where the web bended too much and collided with the screw heads, the aim in this test is to position the profiles in a way that they are only bended in the opposite direction of the screw heads and that the “foot rolls" forwards and presses the frame back.

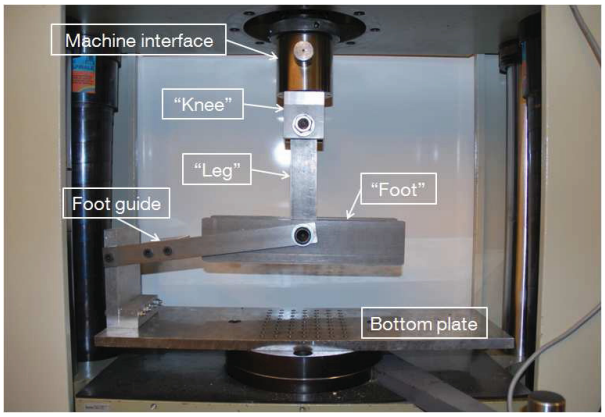

BILD 15. Test set-up of the “step” test

For the specimens without viscoelastic layer the first two of four are placed directly beneath the “leg” (position 0) and the other two are loaded 20 mm right of the first position (position 1). BILD 16 shows the behavior of the second profile without viscoelastic layer during the “step" test in the first position. Corresponding to the second curve in BILD 17, the foot first touches the upper flange and bends it down. Then the web is loaded and bended by a nearly vertical force, leading to the failure of the lower edge and a backward movement of the web. This deflection results in a new stability of the web, supported by the bottom plate, another increase of the foot force and a further failure of the web next to the lower edge from the bottom up. Resulting from the growing distance between the center line of the foot and the web, the moment causes the final failure of the web directly under the upper edge.

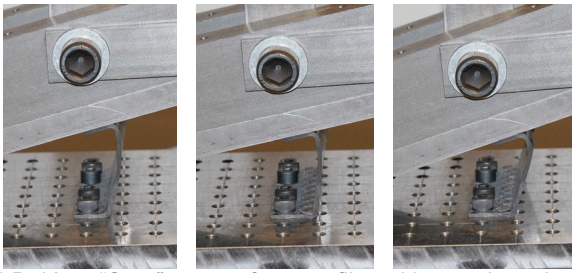

BILD 16. “Step” test of a profile without viscoelastic layer in position 0

Although the first frame piece is not fixed in a way that the foot stepped on the whole upper flange (therefore it is called unsymmetric), it behaved quite similar to the second one, described before. The only difference is that after the failure of the lower edge and the web, the new loading on the web does not lead to a failure of the web under the upper edge, but at a certain point the foot tipped forwards, the specimen backwards and the test stopped.
This also happened with the first profile in the second position.
Opposite to the first profile, the second test in the second position stopped because of a real failure of the specimen. This resulted from the fact, that although the foot tipped forwards after the failure of the lower edge, the specimen did not tip backwards, but was loaded until the web failed under the upper edge.

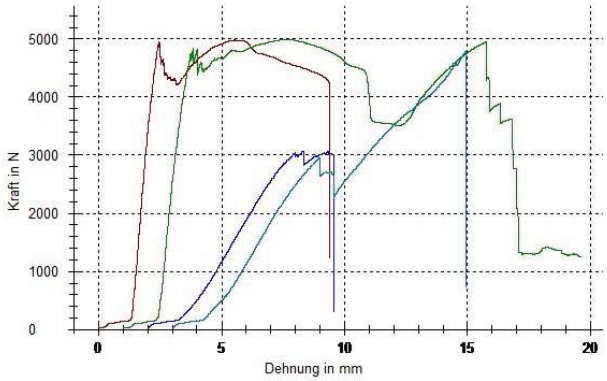

BILD 17. Force-strain diagram of the “step” test with profiles without viscoelastic layer

TAB 3 contains the Young's modulus or respectively the spring rate, the maximum force and the strain at the maximum force of the step test specimen. The values of the spring rate highly depend on the position of the specimen relative to the foot, but show equal values for the same configuration. The maximum forces are similar except for the first specimen in position 1 and indicate the absolute maximum force under which a frame piece of 100 mm width without viscoelastic layer fails, independently on the exact position and orientation of the applied load.

Specimen	Young’s modulus	Maximum force
Position 0, unsym	5285 N/mm	4978 N
Position 0, sym	5132 N/mm	4986 N
Position 1	718 N/mm	3072 N
Position 1	723 N/mm	4794 N

TAB 3. Young’s modulus and maximum force of the “step” test with profiles without viscoelastic layer

In case of the specimens with viscoelastic layer, the first and the last one are investigated in position 0, the second one was placed in position 1 and the third one in position 2. BILD 18 shows the behavior of the first frame piece in position 0. First the upper flange was bended down, as in case of the undamped frames. But then the load on the web and the resulting bending caused a crack between the upper and the lower layers of the web at the lower end of the viscoelastic layer and a separation of the upper layers from the viscoelastic layer up to the center of the web. In the next step the inner layer at the upper end of the viscoelastic layer failed and at last the outer layer failed at the same position.

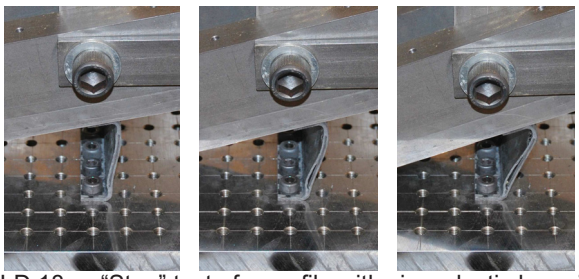

BILD 18. “Step” test of a profile with viscoelastic layer in position 0

The fourth profile, which is also loaded in position 0, showed a slightly different behavior, because here the load caused first the failure of the inner web layer at the upper end of the viscoelastic layer and then the separation of the inner layers of the web started form the upper end, but results in almost the same force-strain diagram in BILD 19.
The load on the specimen in position 1, that corresponds to the second graph in BILD 19, first caused the usual down bending of the upper flange. But then with rising force, the web tipped backwards, the foot tipped forwards and the test continued by transferring the load of the foot only to the upper end of the flange. In this way the whole not deformed web and upper flange were bended around the lower edge until it failed.
In position 2, the foot tipped until it reached the upper end of the flange with its lower surface and the bottom plate with its forward end. Then the upper flange was first bended down and then the web was loaded. The further steps correspond to the first profile, because the bending of the web caused first a crack between the inner and outer layers of the web at the lower end of the VEL. Then the inner layers separated from the VEL from the bottom up, resulting in a failure of the inner layers at the upper end of the viscoelastic layer. The final failure of the outer layers at the upper end of the viscoelastic layer was equal to the final failures of both specimens in position 0.

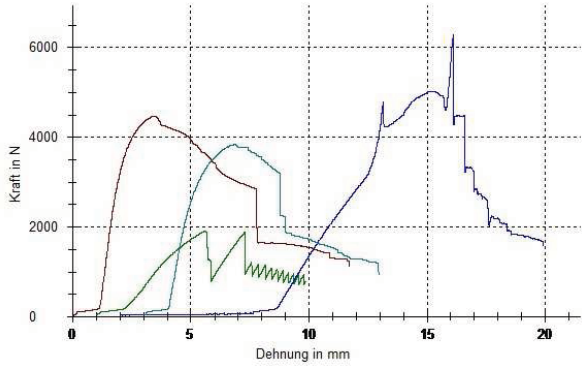

BILD 19. Force-strain diagram of the “step” test with profiles with viscoelastic layer

TAB 4 summarizes the Young's modulus, the maximum force and the strain at the maximum force of the specimens of the profile with viscoelastic layer. First, the results of the two specimens in position 0 indicate that the profiles with viscoelastic layer do not show the same behavior as the profiles without viscoelastic layer, because both the spring rate and the maximum force are quite different, corresponding to the different behavior, described above. The extremely high maximum force in case of position 2 may result from the fact that in this case the web was loaded by a lower load and in a more vertical manner than the profiles in position 0, because of the fact that the foot not only touched the upper flange, but also the bottom plate with its tip.

Specimen	Young’s modulus	Maximum force
Position 0	3938 N/mm	4469 N
Position 1	669 N/mm	1913 N
Position 2	846 N/mm	6275 N
Position 0	2743 N/mm	3849 N

TAB 4. Young’s modulus and maximum force of the “step” test with profiles with viscoelastic layer

Compared to the results of the profiles without viscoelastic layer, the profiles with viscoelastic layer show higher differences in their results for the same test and a lower strength and stiffness, because both the spring rates and the maximum forces are smaller for position 0 and 1.

7. NUMERICAL ANALYSES

Based on the FE model of chapter 3 the carbon fiber reinforced polymer C-frame is modeled with and without integrated viscoelastic layer. To be able to compare simulation and test results the harmonic analysis is performed in the same frequency range (200 Hz to 1000 Hz) as the vibro-acoustic rating test.

7.1. Comparison of the Test and the Simulation Results

The lower figure in BILD 20 shows the frequency response function of the FE model of the C-frame with viscoelastic layer for the web, the left and the right flange, calculated from the displacement output of the harmonic analysis. Furthermore the figure indicates the loss factors for all relevant modes, calculated with MATLAB by the “n dB" method. The figure above from chapter 6.1 contains the frequency response function of the tested profile with viscoelastic layer.
Comparing the shape of the both frequency response functions shows that they are qualitatively the same because they have the same number and positions of the resonance frequencies to one another. The differences are that the corresponding modes of the harmonic are between 15 Hz for mode 5 and 38 Hz for mode 3 of the simulation higher than the test frequencies, except for the last mode 6, which is 32 Hz lower than the corresponding test mode.
These mode deviations result either from the different material properties or from geometric model inaccuracies, that have a great influence on the eigenfrequencies, as previous results implied, and which are possible because the model uses the theoretical measures and not the one of an actual manufactured profile with its shrinkage and geometrical variations. Another reason for the mode deviations can be related to the fact that all loss factors of the simulation results are much smaller than the ones evaluated in the tests. This might be caused by the fact that the material loss factor of the CFRP is not known and therefore not included into the simulation model, but the high loss factors of the profile without viscoelastic layer indicate that the material loss factor may not be neglected.

The assumption of chapter 6.1 that the second mode of the profile without viscoelastic layer corresponds to the highly damped mode at 646 Hz, can be validated with the result of the harmonic analysis, because the kind of resonance at 711 Hz, where the peak of the web frequency response function surpasses the frequency response function of the left and the right flange, correlates with this mode. The explanation is that at this frequency the web is more excited than both two flanges, although the shaker actively excites only the right flange, and therefore the loss factor is much higher, because the higher excitation of the web leads to a higher deformation of the viscoelastic layer.

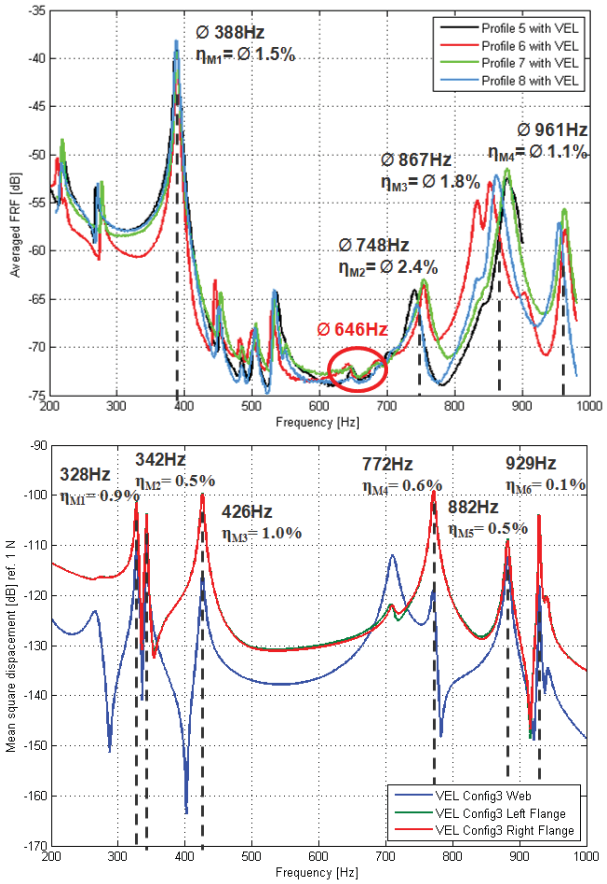

BILD 20. Frequency response function of the vibration test (above) and of the FE model of the frame with viscoelastic layer (below)

7.2. Mode Identification

To be able to further analyze the modes of the left flange BILD 21 to BILD 24 present the images of the displaced structure from ANSYS.
The first two modes in BILD 21 seem to show the first torsion mode of the web, where the lower mode at 328 Hz might be combined with the second bending mode of the excitation part. This is also indicated by the fact that the maximum displacements of this mode are smaller than the ones for the mode at 342 Hz.

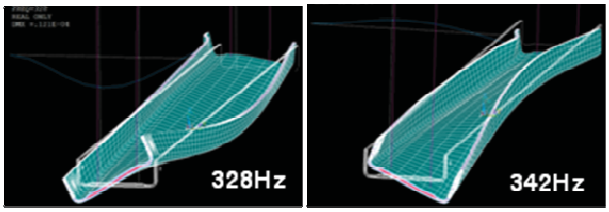

BILD 21. Three-dimensional image of the first (left) and the second mode (right)

The left picture of BILD 22 displays the first main mode of the flanges, looking like the first bending mode about the y-axis. Due to the fact that the left and the right flange bend in opposite directions the web is not strongly deformed, resulting in a relatively low loss factor.
As already assumed before, the right picture of BILD 22 contains the proof that at 711 Hz mainly the web is excited to vibrate in its second bending mode, resulting in the high damping effect.

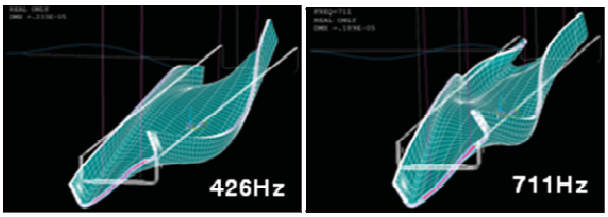

BILD 22. Three-dimensional image of the third (left) and the fourth mode (right)

The fifth mode in the left picture of BILD 23 shows the combination of the second bending mode of the flanges around the y-axis and the torsion of the web. The torsion causes shear deformation in the viscoelastic layer and therefore a comparably high loss factor.
The right picture of BILD 23 displays the second bending mode of the whole frame. Due to the tension in the viscoelastic layer it damps, but not as much as in the previous mode, because the shear deformation is smaller.

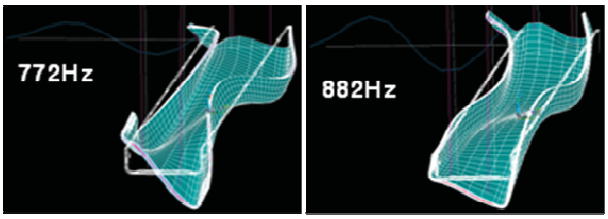

BILD 23. Three-dimensional image of the fifth (left) and the sixth mode (right)

The last mode in BILD 24 looks like the second bending mode of the left flange around the z-axis. Therefore the web is nearly not deformed and the resulting damping improvement by the viscoelastic layer is nearly negligible.

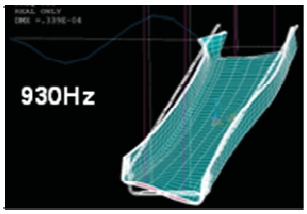

BILD 24. Three-dimensional image of the seventh mode

8. CONCLUSIONS AND OUTLOOK

The aim of MAAXIMUS is to find a trade-off between meeting the requirements on a composite aircraft fuselage in the 21st century and its development and manufacturing costs. The objective of this work was to investigate the static and dynamic properties of C-frames with integrated viscoelastic layer for extending their functionality by the ability to damp vibrations.
The dynamic analysis of a thin-walled open aluminum beam with free-free boundary conditions revealed that two suspension configurations are required for investigating all response mode shapes. Furthermore the related numerical analysis showed that the finite element model updating with the modal strain energy method does not improve the correlation of the simulation results in the same way as for more simple geometries. This observation should be validated and further investigated by means of the finite element model of the carbon fiber reinforced polymer profiles.
The new design of the RTM tool enabled the manufacturing of valuable C-frames and provides also the possibility to further investigate the main parameters of the resin injection.
The static tests showed different results. In the specially developed “step" test the profile with viscoelastic layer performed worse than the profile without viscoelastic layer. Additionally, the specimens of the damped C-frame show higher differences in terms of the maximal force and their failure behavior. However, the four-point bending test revealed higher mechanical properties for the profile with viscoelastic layer, resulting from a 22% higher torsional stiffness and a 10% higher bending strength of the web.
The dynamic tests of the carbon fiber reinforced polymer C-frames indicated that the viscoelastic layer does not noticeably improve the overall damping performance. Especially in the configuration representing its real operation behavior, the first mode is damped 20% less and the further modes show a damping increase of up to 20%, while the mass of the profile is increased of 12%. Further investigations should aim at the increase of deformation in the damping treatment either by changing the position of the viscoelastic layer or adapting the C-frame. The prepared finite element models should serve as basis for this purpose.

References

[1] www.maaximus.eu, Maaximus 2009

[2] Christensen, Richard M.: Theory of Viscoelasticity, Dover Publications, New York, USA, 1982

[3] Ungar, Eric E.; Kerwin, Edward M. Jr.: Loss Factors of Viscoelastic Systems in Terms of Energy Concepts, In: The Journal of the Acoustical Society of America 34(7/1962), pp. 954-957

[4] Johnson, Conor D.; Kienholz, David A.; Rogers, Lynn C.: Finite Element Prediction of Damping in Beams with Constrained Viscoelastic Layers, In: Shock and Vibration Bulletin 51(1/1981), pp. 71-80

[5] ASTM International: Standard Test Method for Measuring Vibration-Damping Properties of Materials, Designation E 765-05, West Conshohocken, USA, October 2005

[6] Lepoittevin, Gregoire: Finite element model updating of vibrating structures under free-free boundary conditions for modal damping prediction, PhD-Seminar 2009, Center of Structure Technologies, ETH Zurich